Single-molecule surface-enhanced Raman spectroscopy of 4,4'-bipyridine on a prefabricated substrate with directionally arrayed gold nanoparticle dimers

Sugano, Koji
Aiba, Kiyohito
Ikegami, Kohei
Isono, Yoshitada

(Citation)
Japanese Journal of Applied Physics,56(6S1):06GK01-06GK01

(Issue Date)
2017-06

(Resource Type)
journal article

(Version)
Accepted Manuscript

Single-molecule surface-enhanced Raman spectroscopy of 4,4'-bipyridine on a prefabricated substrate with directionally arrayed gold nanoparticle dimers

Koji Sugano*, Kiyohito Aiba, Kohei Ikegami, and Yoshitada Isono

Department of Mechanical Engineering, Graduate School of Engineering, Kobe University, Kobe 657-8501, Japan

*E-mail: sugano@mech.kobe-u.ac.jp

In this study, single-molecule detection on a prefabricated substrate through surface-enhanced Raman spectroscopy (SERS) with 4,4'-bipyridine molecules was achieved. The use of a substrate with directionally arrayed gold nanoparticle dimers was proposed for the single-molecule detection and identification of a wide range of bio/chemical molecules. Around 50 Raman measurements and statistical analyses were performed to demonstrate a single-molecule SERS. At 10^{-11} M, the distribution was fitted by three Gaussian curves, whereas the distribution of Raman intensities was fitted by one Gaussian curve at 10^{-5} M. The probability of molecule detection is consistent with the Poisson distribution. This result indicates the possibility of detecting 0, 1, and 2 molecules. Thus, we confirmed that the developed substrates achieved single-molecule SERS detection and identification.

1. Introduction

In recent years, a highly sensitive molecule detection of extremely low molecular concentration has been used for various fields such as medicine, biology, and environment.[1-5] Its medical and biology applications include the detection of biomolecules such as metabolites, proteins, and DNA bases. Its environmental application includes the chemical detections of residual pesticides, explosive substances, and environmental detrimental substances. For these trace analyses, surface-enhanced Raman spectroscopy (SERS) has been expected because it has the potential to highly sensitively detect and identify molecules. Raman spectroscopy is a powerful tool for molecular identification because a Raman spectrum includes molecular structural information. The Raman scattering light from a small number of molecules is significantly weak. In SERS, however, the Raman scattering light can be enhanced by plasmonic resonance, which is generated on metal nanostructure surfaces.[1,6] Therefore, SERS analysis enables us to perform the high-sensitivity rapid detection and reliable identification of bio/chemical molecules without labeling, including single-molecule detection and identification.[7-10]

As a metal nanostructure for SERS on a substrate, numerous reports have been reported thus far. Most of the reported structures have been fabricated by self-organization processes. The fabrication procedures used are categorized into two methods, namely, (i) in-liquid formation[7-10] and (ii) on-substrate fabrication.[4,11-13]

In the formation method (i), an analyte solution and a colloidal nanoparticle solution are mixed so that particles form particle dimers or agglomerates in liquid with a molecular bridge between particles. The particles gap is less than 1 nm. This nanogap results in a marked Raman enhancement because it exponentially increases as the nanogap decreases. The mixed solution is used for in-liquid SERS measurement, or is placed and dried on a substrate followed by on-substrate SERS measurement. In this manner, single-molecule detection has been reported using the dimer configuration obtained when the polarization direction of an incident light is matched to a particle-particle connection direction.[9,10] Many theoretical studies have supported this polarization-dependent Raman enhancement.[14,15] In this method, the following problems emerge depending on the applications. One problem is that long-time incubation is required after mixing the analyte and colloidal solutions for dimer or agglomerate formation. Therefore, the SERS substrate obtained by on-substrate

fabrication (ii) is suitable for practical applications of single-molecule SERS. Another problem is that the connection direction cannot be controlled on a substrate for on-substrate SERS measurement.[10,14] Thus, it is necessary to adjust the polarization direction to the connection direction of particles after a scanning electron microscopy (SEM) or an atomic force microscopy (AFM) observation for each SERS structure.

For a prefabricated SERS substrate obtained by the formation method (ii), self-organized methods such as particle aggregation,[4,11] carbon nanotube (CNT) aggregation,[12] and nanoporous fabrication[13] on a substrate have been reported. The structures involved in these method include numerous nanogaps called hotspots. The polarization-dependent property of Raman enhancement, however, has been unconcerned. Structures with a large effect on the Raman enhancement factor are randomly formed, and the induction probability of the marked enhancement is extremely low. Therefore, the self-organized structures result in sensitivity and reliability limitations especially for low-concentration trace detection and single-molecule analysis.

In this study, we propose the SERS structure shown in Fig. 1, which shows a high sensitivity for single-molecule SERS analysis. The SERS structure consists of gold nanoparticle dimers that are directionally arrayed on a substrate for a marked electromagnetic enhancement. It is fabricated by nanotrench-guided self-assembly with a high yield.[16-18] It enables us to utilize the effect of polarization on the enhancement for single-molecule SERS. Although electron beam (EB) lithography or focused ion beam (FIB) has been used for fabricating orderly nanostructures, it cannot be used for fabricating a nanogap of around 1 nm, which shows a marked electromagnetic enhancement.

In this paper, the method of fabricating the proposed substrate and single-molecule detection using 4,4'-bipyridine molecules by the statistical analysis of Raman intensities are reported. As a SERS probe for single-molecule SERS studies, probe molecules with large Raman cross sections, such as rhodamine 6G (RH6G) and crystal violet (CV) have been used.[19] In this study 4,4'-bipyridine molecules were used; these molecules have been introduced as molecules with small Raman cross sections in the literature.[20,21]

2. Experimental and analytical methods

2.1 Proposed structure

We proposed the use of directionally and regularly arrayed gold nanoparticle dimers as the SERS substrate shown in Fig. 1. In this study, gold nanoparticles with mean particle diameters of approximately 100 nm were arrayed on a Si substrate by a nanotrench-guided self-assembly. The effect of SERS on particle diameter has been investigated.[22,23] A common finding is that the Raman intensity increased with particle diameter up to 100 nm, as indicated in Refs. 22 and 23. Although the quadrupole mode appears for larger particles, the dipole mode is dominant for 100 nm particles. The nanoparticles are arranged along the template nanotrenches so that the connection direction of the arranged particles is easily matched to the polarization direction of the incident light without SEM and AFM observations.

2.2 Fabrication method

The nanotrench-guided self-assembly used in this study is shown in Fig. 2. A colloidal nanoparticle solution was injected between a cover glass and a template substrate of Si with an array of nanotrenches fabricated by EB lithography and dry etching. On drying the aqueous particle dispersion between the substrates, the water surface line moved backward and the particles became concentrated near the edge of the meniscus. The drag force pressed the particles onto the template substrate. When the meniscus passed over the templates, the particles were trapped on the template nanotrenches. Then, the water-bridge force acted on the trapped particles during drying, connecting the particles to each other.

The gold nanoparticles were synthesized by a citrate reduction method. The synthesized particles showed negatively charged surfaces because acetonedicarboxylic acid and acetoacetictic acid molecules uniformly formed and attached to particle surfaces without vacancy during synthesis.[24,25] Nanoparticle aggregation was minimized by electrostatic repulsion between the nanoparticles.

During the removal of the remaining water between the particles, the particles attracted each other and formed particle–particle contacts, which acted as hotspots. A nanogap of around 1 nm formed between the nanoparticles because the molecules attached to the surfaces acted as spacers. The fabricated structures were used for SERS measurements after removing the attached molecules by UV/O_3 treatment.

Figure 3 shows the SEM images of the fabricated nanostructures. We observed that gold nanoparticles were arranged onto the nanotrench template and gold nanoparticle dimers were

arrayed directionally and regularly. Although the length of the nanotrench was 260 nm, two particles with a mean dimeter of 100 nm were connected by water bridge force during the drying process.

2.3 Simulated electromagnetic enhancement

We performed an electromagnetic simulation using the commercially available finite-difference time-domain (FDTD) simulation software. The simulation was carried out using a three-dimensional model with 400 and 300 nm lengths for the x- and y-axes, respectively. A gold nanoparticle dimer was placed at the center of the x- and y-axes on a Si substrate. The diameter and gap between particles were 100 and 1 nm, respectively. We used CRC and Palik data for the refractive indices of Au and Si, respectively, which are available in the software. Periodic boundary conditions along the x- and y-axes, and perfectly matched layers (PML) along the z-axis were used. A plane wave source was set with a wavelength range of 400–800 nm. A 0.2 nm mesh size was used for the nanogap area. We obtained electromagnetic field enhancement factors $|E|^2$ at a nanogap.

Figure 4(a) shows the simulated spectra of the electromagnetic field enhancement factor as a function of polarization angle at the hotspot of two particles. The enhancement factor decreased with increasing the polarization angle. The proposed structure was observed to be suitable for SERS with the 632.8 nm laser used in this study. Figure 4(b) shows the contour plots of electromagnetic field enhancement. The incident light was localized at a nanogap between particles in both cases of polarization angles of 0 and 90 degrees in the simulation. The electromagnetic field enhancement factors at the nanogap for the polarization angles of 0 and 90 degrees were around 1.1×10^2 and 3.5×10^5 times at the incident light wavelength of 632.8 nm, respectively, indicating a ratio of around 3.3×10^3 times. This result indicates that directionally arrayed dimer structures are expected to induce a marked Raman enhancement compared with randomly arranged structures.

3. Results and discussion

A 632.8 nm laser-equipped micro-Raman spectrometer was used in this study. As a target molecule of detection, 4,4’-bipyridine was used, which is a pesticide material.

We performed around 50 Raman measurements for each measurement time (1 or 0.05 s) and molecule concentration (10^{-5} or 10^{-11} M). Figure 5 shows some examples of the obtained

spectra. Dotted lines indicate the Raman shifts derived from 4,4'-bipyridine.[26] Then, statistical analysis was performed as shown in Fig. 6. The relative Raman intensities were calculated using the average Raman intensity for each condition. All spectra were discriminated on the basis of the presence (red column) or absence (blue column) of a peak at around 1609 cm^{-1} that corresponded to the Raman shift of the target molecule.

At a 10^{-5} M concentration, all spectra exhibited clear peaks in both cases of measurement times (1 and 0.05 s). The distribution of Raman intensities was fitted by one Gaussian curve as shown in Figs. 6(a-1) and 6(a-2). At a 10^{-11} M concentration, the spectra with and without Raman peaks were observed as shown in Fig. 5. The experimental data at 1 and 0.05 s were fitted by three and two Gaussian curves, respectively as shown in Figs. 6(b-1) and 6(b-2). Since the first frequency peak in Figs. 6(b-1) and 6(b-2) comprises a data set without Raman peaks (blue columns), it is treated as a background intensity. It is considered that the second and third peaks in Fig. 6(b-2) correspond to the data sets of 1 and 2 molecules detection, respectively, for the measurement time of 1 s. The average relative intensities of 0, 1, and 2 molecules were 0.89, 1.06, and 1.28 at 1 s, respectively. The net relative intensity of 2 molecules was calculated to be 1.28−0.89=0.39, which is 2.3 times as high as that of 1 molecule (1.06−0.89=0.17).

Then, the Poisson distribution was calculated for each measurement time as shown in Table I. The experimental statistical distribution was consistent with the Poisson distribution. At the detected molecular number of 3 at the integration time of 1 s, the calculated frequency in the Poisson distribution was 0.7. The experimental frequency of 0 was relevant. The experimental frequencies at 0.05 s were also relevant to the detected numbers of 2 and 3. The statistical distribution at 10^{-11} M was explained by the Poisson distribution. The frequency of the second peak decreased with decreasing measurement time from 1 to 0.05 s as shown in Figs. 6(b-1) and 6(b-2). These results indicate that a single molecule was stochastically detected.

We calculated the Raman enhancement factor. The experimental Raman enhancement factor was calculated as $EF = (I_{SERS}/C_{SERS})/(I_{non-SERS}/C_{non-SERS})$. Here, I and C are Raman intensities per integration time and concentration, respectively. The subscripts *SERS* and *non-SERS* indicate the presence and absence of nanostructures, respectively. The measured Raman intensity without nanostructures was 2.0 counts/s at the concentration of

10^{-2} M and the integration time of 100 s for the Raman shift of 1609 cm^{-1}. The Raman enhancement factors calculated from the experimental results were 9.0×10^{11} and 1.0×10^{12} at the integration times of 1 and 0.05 s, respectively.

The simulated Raman enhancement factor was 6.3×10^{10} at 1609 cm^{-1}, calculated by $|E_I|^2 \times |E_R|^2$ according to the spectrum of the electromagnetic enhancement shown in Fig. 4. Here, $|E_I|^2$ and $|E_R|^2$ are the electromagnetic enhancement factors at the wavelengths of the incident light (632.8 nm) and Raman scattering light (704 nm corresponding to 1609 cm^{-1}), respectively. Note that the experimental Raman enhancement includes the chemical enhancement due to charge transfer between a molecule and a gold surface in addition to the electromagnetic enhancement. It has been reported to be 10–100.[27-31] Therefore, the total Raman enhancement is 6.3×10^{11}–6.3×10^{12} in the calculation. The Raman enhancement factors calculated from the experimental results are consistent with the simulation result.

The bare Raman cross sections of RH6G and CV have been reported to be on the order of 10^{-26}–10^{-27} cm^2/sr.[19] For a pyridine molecule, the bare Raman cross section is on the order of 10^{-29} cm^2/sr.[29-31] The chemical enhancement factors of both molecules are on the same order.[32] Therefore, the fabricated SERS structure in this study was proven to show a marked Raman enhancement. The minimum Raman cross section of bio/chemical substances and the actual cross section necessary to single-molecule SERS are on the orders of 10^{-30} and 10^{-20} cm^2/sr, respectively.[19] Therefore, the total Raman enhancement factor of 1.0×10^{12} obtained in this study is considerably sufficient for the single-molecule SERS of a wide variety of bio/chemical substances.

4. Conclusions

In this study, we fabricated directionally arrayed gold nanoparticle dimers in order to achieve a marked Raman enhancement, and evaluated the structures experimentally for single-molecule SERS using 4,4'-bipyridine molecules. The dimer array was fabricated on a Si substrate by the nanotrench-guided self-assembly of 100-nm-diameter gold nanoparticles. We confirmed the high-yield arrangement of the particle dimers with hotspots in one direction. The fabricated structure showed a high sensitivity with a 10^{-11} M and 0.05 s limit of detection. Then, around 50 Raman measurements and statistical analyses were performed. At 10^{-5} M, the distribution of Raman intensities was fitted by one Gaussian curve. At 10^{-11}

M, the distribution was fitted by three Gaussian curves. This distribution is consistent with the Poisson distribution. This indicates the probability of detecting 0, 1, and 2 molecules. From these results, we confirmed that the developed substrates achieved single-molecule SERS detection and identification. The calculated Raman enhancement factor was 1.0×10^{12}, which is consistent with the estimation result. The Raman enhancement factor is thought to be sufficient for the single-molecule detection of a wide variety of bio/chemical molecules.

Acknowledgments

The Raman spectroscopy experiments were performed at the Kyoto Integrated Science and Technology Bio-Analysis Center (KIST-BIC), sponsored by the Japan Science and Technology Agency (JST). Part of this study was supported by the Kyoto University Nano Technology Hub in the “Nanotechnology Platform Project”, sponsored by the Ministry of Education, Culture, Sports, Science, and Technology, Japan (MEXT). This work was supported by the Japan Society for the Promotion of Science (JSPS) KAKENHI Grant Number 24510138, Grant-in-Aid for Scientific Research (C).

References

1) D. Cialla, A. März, R. Böhme, F. Theil, K. Weber, M. Schmitt, and J. Popp, Anal. Bioanal. Chem. **403**, 27 (2012).
2) K. Kneipp, H. Kneipp, I. Itzkan, R. R. Dasari, and M. S. Feld, Curr. Sci. **77**, 915 (1999).
3) C. Otto, T. J. J. van den Tweel, F. F. M. de Mul, and J. Greve, J. Raman Spectrosc. **17**, 289 (1986).
4) P. C. Pinheiro, S. Fateixa, H. I. S. Nogueira, T. Trindade, J. Raman Spectrosc. **46**, 47 (2015).
5) S. E. J. Bell and N. M. S. Sirimuthu, J. Am. Chem. Soc. **128**, 15580 (2006).
6) S. -C. Luo, K. Sivashanmugan, J. -D. Liao, C. -K. Yao, and H. -C. Peng, Biosens. Bioelectron. **61**, 232 (2014).
7) P. G. Etchegoin and E. C. Le Ru, Phys. Chem. Chem. Phys. **10**, 6079 (2008).
8) K. Kneipp, Y. Wang, H. Kneipp, L. T. Perelman, I. Itzkan, R. R. Dasari, and M. S. Feld, Phys. Rev. Lett. **78**, 1667 (1997).
9) K. Kneipp, H. Kneipp, V. B. Kartha, R. Manoharan, G. Deinum, I. Itzkan, R. R. Dasari, and M. S. Feld, Phys. Rev. E **57**, R6281 (1998).
10) S. Nie and S. Emory, Science **275**, 1102 (1997).
11) R. G. Freeman, K. C. Grabar, K. J. Allison, R. M. Bright, J. A. Davis, A. P. Guthrie, M. B. Hommer, M. A. Jackson, P. C. Smith, D. G. Walter, and M. J. Natan, Science **267**, 1629 (1995).
12) A. O. Altun, S. K. Youn, N. Yazdani, T. Bond, and H. G. Park, Adv. Mater. **25**, 4431 (2013)
13) H. Liu, L. Zhang, X. Lang, Y. Yamaguchi, H. Iwasaki, Y. Inouye, Q. Xue, and M. Chen, Sci. Rep. **1**, 112 (2011).
14) K. Yoshida, T. Itoh, H. Tamaru, V. Biju, M. Ishikawa, and Y. Ozaki, Phys. Rev. B **81**, 115406 (2010).
15) H. Xu, J. Aizpurua, M. Käll, and P. Apell, Phys. Rev. **62**, 4318 (2000).
16) K. Sugano, T. Ozaki, T. Tsuchiya, and O. Tabata, Sens. Mater. **23**, 263 (2011).
17) T. Ozaki, K. Sugano, T. Tsuchiya, and O. Tabata, J. Microelectromech. Syst. **16**, 746 (2007).
18) K. Sugano, K. Suekuni, T. Takeshita, K. Aiba, and Y. Isono, Jpn. J. Appl. Phys. **54**, 06FL03 (2015).
19) E. C. Le Ru, E. Blackie, M. Meyer, and P. G. Etchegoin, J. Phys. Chem. C **111**, 13794 (2007).

20) X. Wang, Z. Liu, M.-D. Zhuang, H.-M. Zhang, X. Wang, Z.-X. Xie, D.-Y. Wu, B. Ren, and Z.-Q. Tian, Appl. Phys. Lett. **91**, 101105 (2007).
21) Z. Liu, X. Wang, K. Dai, S. Jin, Z.-C. Zeng, M.-D. Zhuang, Z.-L. Yang, D.-Y. Wu, B. Rena, and Z.-Q. Tiana, J. Raman Spectrosc. **40**, 1400 (2009).
22) P. P. Fang, J.-F. Li, Z.-L. Yang, L.-M. Li, B. Ren, and Z.-Q.Tian, J. Raman Spectrosc. **39**, 1679 (2008).
23) P. N. Njoki, I-I. S. Lim, D. Mott, H.-Y. Park, B. Khan, S. Mishra, R. Sujakumar, J. Luo, and C.-J. Zhong, J. Phys. Chem. C **111**, 14664 (2007).
24) C. H. Munro, W. E. Smith, M. Garner, J. Clarkson, and P. C. White, Langmuir, **11**, 3712 (1995).
25) K. Sugano, Y. Uchida, O. Ichihashi, H. Yamada, T. Tsuchiya, and O. Tabata, Microfluid. Nanofluid. **9**, 1165 (2010).
26) S. -W. Joo, Vib. Spectrosc. **34**, 269 (2004).
27) A. Campion and P. Kambhampati, Chem. Soc. Rev. **27**, 241 (1998).
28) A. Campion, J. E. Ivanecky III, C. M. Child, and M. Foster, J. Am. Chem. Soc. **117**, 11807 (1995).
29) B. N. J. Persson, Chem. Phys. Lett. **82**, 561 (1981).
30) X. Jiang and A. Campion, Chem. Phys. Lett. **140**, 95 (1987).
31) D.Y. Wu, M. Hayashi, S.H. Lin, and Z.Q. Tian, Spectrochim. Acta Part A **60**, 137 (2004).
32) W. E. Doering and S. Nie, J. Phys. Chem. B **106**, 311 (2002).

Figure Captions

Fig. 1. Overview of proposed and developed SERS substrate with directionally arrayed dimers, which is prefabricated by nanotrench-guided self-assembly.

Fig. 2. Nanotrench-guided self-assembly. As the colloidal gold solution (mean diameter: 100 nm) is drying, the meniscus moves backward and then particles are trapped by interfacial force onto nanotrenches.

Fig. 3. SEM image of directionally and regularly arrayed gold nanoparticle dimers in (a) 5 × 5 μm^2 whole and (b) magnified areas.

Fig. 4. (Color online) FDTD simulation results for electromagnetic enhancement factor depending on polarization angle θ to the connection direction of two particles. The particle diameter and the gap between the particles were set to 100 and 1 nm, respectively. (a) Spectra show the enhancement factor at a hotspot. The dashed line indicates the wavelength of the incident light used in this study. (b) Contour plot of electromagnetic enhancement factor $|E|^2$ at the polarization angles of 0 and 90° at the wavelength of 632.8 nm.

Fig. 5. (Color online) Raman spectra at molecular concentrations of 10^{-5} and 10^{-11} M with and without peaks. Measurement times of (a) 0.05 and (b) 1 s were used. Dotted lines indicate 4,4'-bipyridine-derived Raman peaks.

Fig. 6. (Color online) Statistical analysis of around 50 SERS measurements. The blue and red columns indicate frequencies without and with a peak at around 1609 cm^{-1}, respectively. The molecular concentration and measurement time are (a-1) 10^{-5} M and 1 s, (a-2) 10^{-5} M and 0.05 s, (b-1) 10^{-11} M and 1 s, and (b-2) 10^{-11} M and 0.05 s, respectively. The data are fitted by Gaussian curves.

Table I. Calculated Poisson distributions and experimental frequencies for the measurement times of (a) 1 and (b) 0.05 s at the molecular concentration of 10^{-11} M.

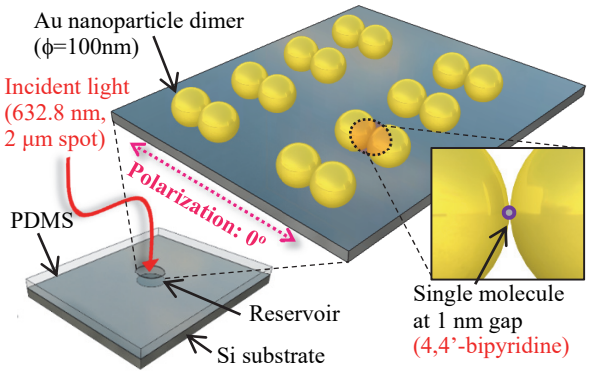

Fig.1. (Color online)

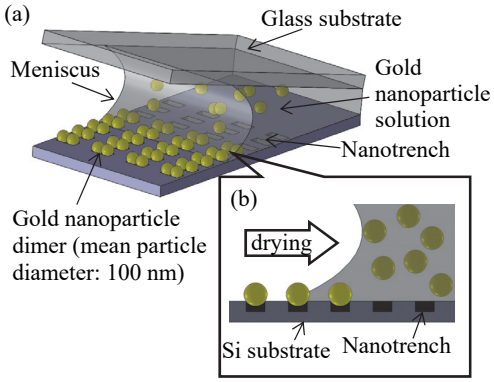

Fig.2. (Color online)

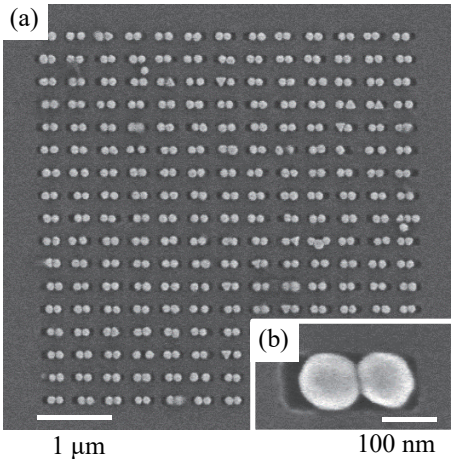

Fig.3.

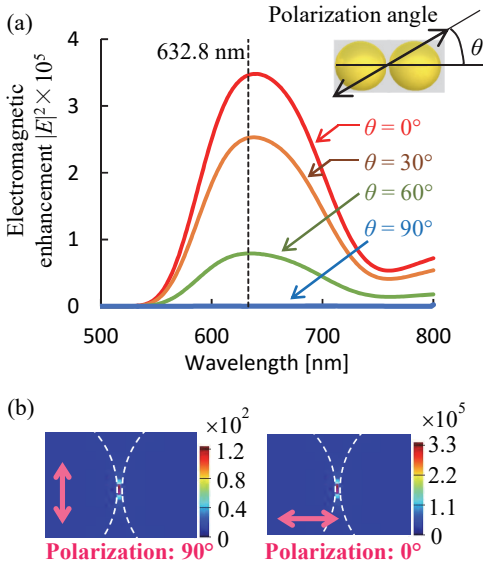

Fig.4. (Color online)

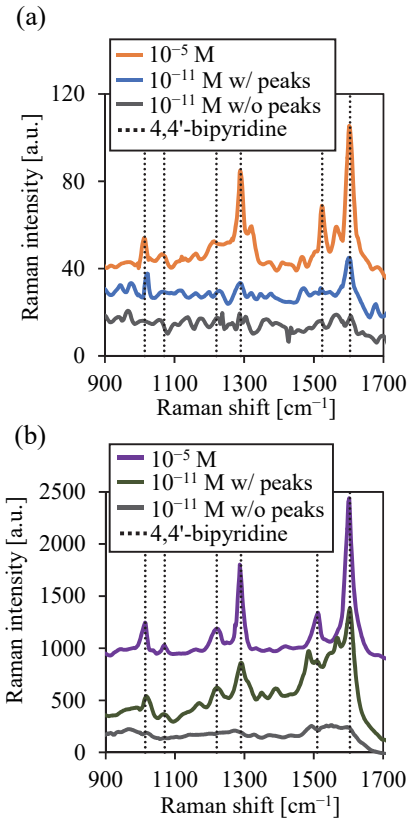

Fig.5. (Color online)

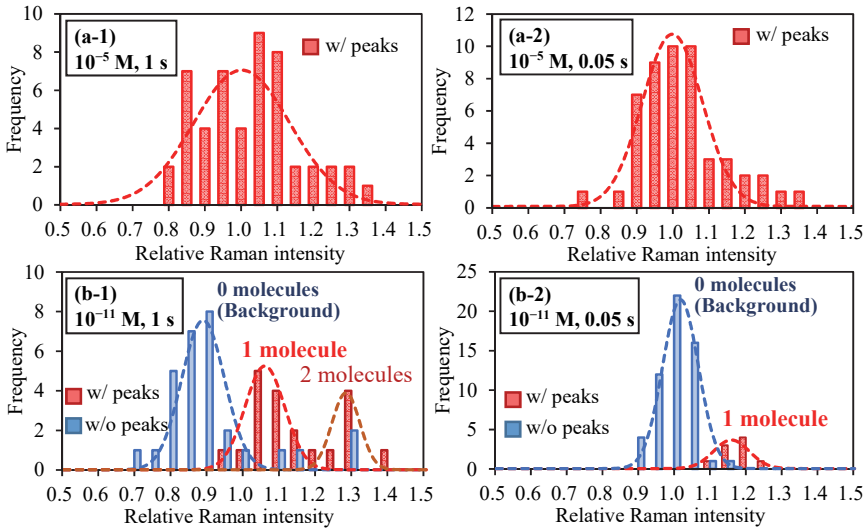

Fig.6. (Color online)

Table I. Calculated Poisson distributions and experimental frequencies for the measurement times of (a) 1 and (b) 0.05 s at the molecular concentration of 10^{-11} M.

(a)

Detected molecular No.	Poisson distribution	Experimental frequency
0	28.8	29
1	15.3	14
2	4.0	6
3	0.7	0

(b)

Detected molecular No.	Poisson distribution	Experimental frequency
0	56.6	56
1	7.8	9
2	0.5	0
3	0.03	0